

펄스레이저 증착법으로 제작된 $\text{Bi}_4\text{Ti}_3\text{O}_{12}/\text{LaAlO}_3$ 박막과 $\text{Bi}_4\text{Ti}_3\text{O}_{12}/\text{YBa}_2\text{Cu}_3\text{O}_{7-x}/\text{LaAlO}_3$ 복합구조의 에피 성장

조월림, 조학주, 노태원
서울대학교 물리학과

Epitaxial Growth of Pulsed-Laser Deposited $\text{Bi}_4\text{Ti}_3\text{O}_{12}/\text{LaAlO}_3$ Thin Films and $\text{Bi}_4\text{Ti}_3\text{O}_{12}/\text{YBa}_2\text{Cu}_3\text{O}_{7-x}/\text{LaAlO}_3$ Heterostructure

W. Jo, H-J. Cho and T. W. Noh
Department of physics, Seoul National University

요 약

펄스 레이저 증착법을 이용하여 강유전체 $\text{Bi}_4\text{Ti}_3\text{O}_{12}$ 박막을 $\text{LaAlO}_3(001)$ 위에 성장시켰다. 넓은 영역의 온도에서 증착한 박막의 상 형성과 구조적 성질을 X선 회절법을 이용하여 조사하였다. 740°C 에서 증착한 박막은 박막의 c -축이 기판에 수직인 형태의 에피 성장의 경향을 보인다. 펄스 레이저 증착법을 이용하여 $\text{Bi}_4\text{Ti}_3\text{O}_{12}/\text{YBa}_2\text{Cu}_3\text{O}_{7-x}/\text{LaAlO}_3$ 복합구조를 *in-situ*로 성장시켰다. $\text{YBa}_2\text{Cu}_3\text{O}_{7-x}$ 의 a -, b -축이 LaAlO_3 와 완벽하게 평행하게 배열되어 있지 않음에도 불구하고, $\text{Bi}_4\text{Ti}_3\text{O}_{12}$ 박막은 에피 성장의 경향을 보인다.

Abstract

Ferroelectric $\text{Bi}_4\text{Ti}_3\text{O}_{12}$ thin films have been grown on $\text{LaAlO}_3(001)$ by pulsed-laser deposition. Phase formation and structural properties of the films prepared at various deposition temperatures are investigated using x-ray diffraction. The film grown at 740°C shows epitaxial growth behavior with c -axis normal to the substrate. Heterostructures of $\text{Bi}_4\text{Ti}_3\text{O}_{12}/\text{YBa}_2\text{Cu}_3\text{O}_{7-x}/\text{LaAlO}_3(001)$ have been *in-situ* grown. Even though the a - and b -axes of the $\text{YBa}_2\text{Cu}_3\text{O}_{7-x}$ layer show epitaxial growth behavior.

1. Introduction

Ferroelectric $\text{Bi}_4\text{Ti}_3\text{O}_{12}$ (BTO) thin films have been recently synthesized by pulsed-laser deposition.¹⁻⁵⁾

BTO is a promising material for a ferroelectric field effect transistor gate, since it has the low coercive field along the c -axis.⁶⁾ BTO is also a good candidate material for electro-optic (EO) waveguide devices,

since it has a high EO coefficient.⁷⁾ In order to obtain a film whose EO coefficient is close to the single crystal value, it is highly desirable to grow the film epitaxially.

To control the physical properties of the BTO film with an external electric field, various materials have been investigated as a proper electrode. Platinum is a frequently used electrode material by many workers⁸⁾, but most films grown on platinum are polycrystalline and susceptible to the problems related to granularity. High temperature superconductors such as $\text{YBa}_2\text{Cu}_3\text{O}_{7-x}$ (YBCO) have been studied as electrode materials for various ferroelectric oxide films, since they provide chemical compatibility and epitaxial growth relationship.⁹⁻¹²⁾

In this study, both BTO thin films and a BTO/YBCO/ $\text{LaAlO}_3(001)$ heterostructure are grown with the pulsed-laser deposition technique. BTO thin films are grown at various substrate temperatures. Even though it is possible to grow the highly oriented BTO films in a relatively wide temperature region, a deposition temperature near 740°C is found to be more desirable. With similar deposition parameters, a BTO/YBCO/ LaAlO_3 structure is grown. Crystal growth behaviors in the BTO thin films and the heterostructure are investigated thoroughly using x-ray techniques.

2. Experiments

Figure 1 shows a schematic diagram of our pulsed-laser deposition system. A visible laser, *i.e.*, second harmonics of a Q-switched Nd:YAG laser, is used in this study. The laser pulse width is 6~7 ns and the repetition rate is 10 Hz. To avoid texturization of a target surface and get a homogeneous film, position of the beam on the target is changed continuously during deposition by

moving a focusing lens. Stoichiometric BTO and YBCO pellets are mounted on a target holder, which can mount up to four targets simultaneously. Using this target holder, it is possible to deposit *in-situ* BTO and YBCO layers for the heterostructure.

Single crystalline $\text{LaAlO}_3(001)$ substrates are carefully prepared with the following procedures: ultrasonic cleaning in an acetone bath for 5 minutes, rinsing in an ethanol bath, and drying with flowing N_2 gas. The cleaned substrates are attached with silver paint on a substrate holder which can be heated up to 850°C using cartridge heaters. The substrate temperature during deposition is measured by two pairs of thermocouples (K-type; Chromel-Alumel) imbedded in the substrate holder.

Details of the deposition conditions for BTO films are given in the second column of Table I. A wide range of the substrate temperature between 640°C and 780°C is used to investigate effects of the deposition temperature on structural properties of the thin films. During the deposition, oxygen pressure of 200 mtorr is maintained by adjusting the oxygen flow rate using feedback signals from a capacitance manometer. Just after deposition, the chamber is rapidly brought up to 500 torr of oxygen, and the film is *in-situ* annealed at 500°C for 30 minutes.

Deposition conditions for a BTO/YBCO/ LaAlO_3 heterostructure are similar to those for the BTO films, as shown in the third and fourth columns of Table I. YBCO layer is first deposited on a $\text{LaAlO}_3(001)$ substrate at 760°C under 200 mtorr of oxygen. Subsequently, the substrate temperature is lowered to 740°C and the BTO film is *in-situ* deposited. Then the chamber is rapidly brought up to 500 torr of oxygen, and the heterostructure is annealed at 500°C for 30 minutes.

Structural properties of the thin films are characterized by x-ray diffraction(XRD) techniques,

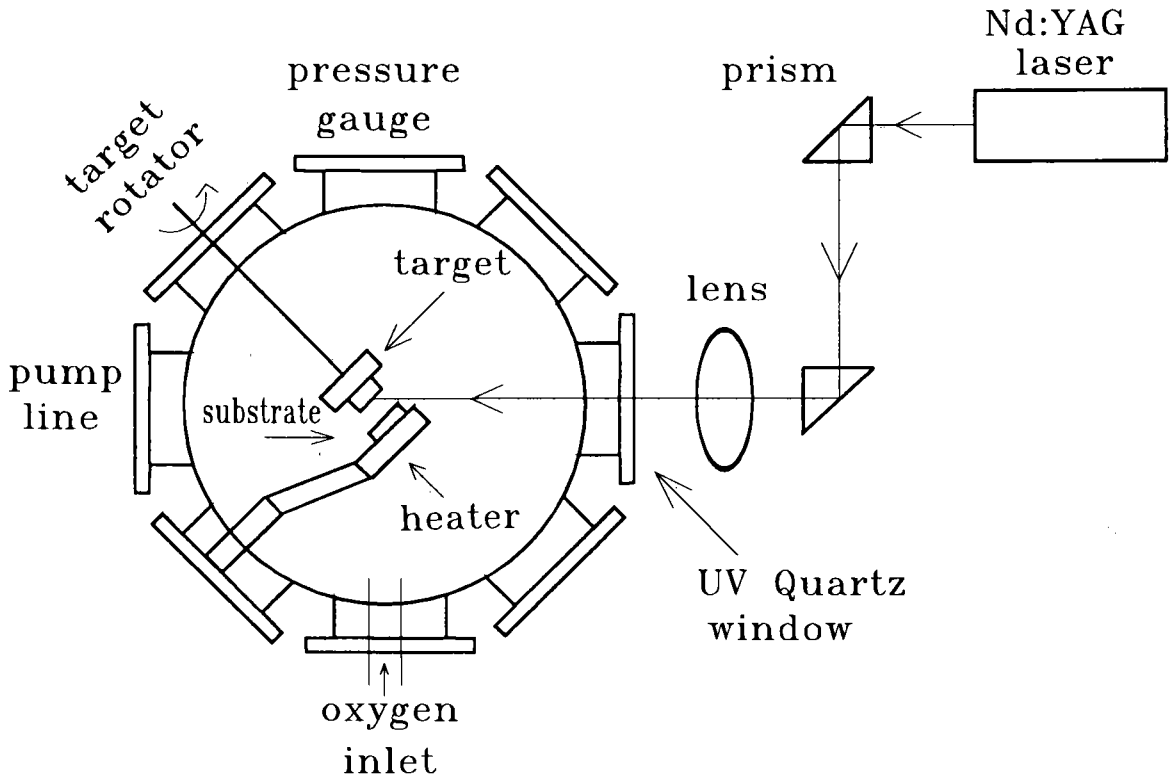


Fig. 1 A schematic diagram of our pulsed-laser deposition system.

Table I. Deposition conditions for BTO thin films and a BTO/YBCO/LaAlO₃ heterostructure.

	BTO films	BTO/YBCO/LaAlO ₃ (YBCO layer)	heterostructure (BTO film)
Deposition temperature	640~780°C	760°C	740°C
Laser fluence	1.5~ 2 J/cm ²	2 J/cm ²	1.5~2 J/cm ²
Oxygen pressure	200 motorr	200 motorr	200 motorr
Annealing condition	500°C and 500 torr of oxygen for 30 minutes		
Typical thickness	3000Å	1000Å	3000Å

including θ - 2θ scan, rocking curve, and x-ray pole figure measurements. Surface morphology and roughness are examined with the atomic force microscopy (AFM).

3. Results and Discussions

Figure 2 shows XRD patterns of the BTO/LaAlO₃(001) films deposited at various temperatures between 640°C and 780°C. The CuK α line is used as an x-ray beam source. As shown in Fig. 2(a), the film deposited at 780°C has strong (00 l) peaks of the perovskite BTO phase. (220) and (642) reflections of Bi-deficient Bi₂Ti₂O₇ phase appear near the (004) and (0012) peaks of the BTO, respectively. Figures 2(b) and 2(c) show the XRD data for the films deposited at 740°C and 700°C, respectively. These films show only (00 l) reflections of the BTO phase. As shown in Figs. 2(d) and 2(e), the films grown below 700°C have (00 l) peaks of BTO phase. The (222) and (662) reflections of Bi₂Ti₂O₇ phase appear near the (006) and (0014) peaks of BTO, respectively. Therefore, the deposition temperature between 700°C and 740°C is required to grow the BTO films without the secondary phase problem. Film grown at this temperature range is composed of grains whose c-axis is normal to the substrate.

The crystallinity of highly c-axis oriented BTO films was examined by x-ray rocking-curve measurements. The (008) reflection of the films grown at 700°C and 740°C was chosen since the peak intensity is so high. [Refer to Fig. 2. The full width at half maximum (FWHM) for the (008) reflection of the film deposited at 740°C is smaller than 0.3°. On the other hand, the FWHM for the film grown at 700°C is about 1°. Therefore, the thin film grown at 740°C is more highly c-axis

oriented than that grown at 700°C.

The lateral registry between the crystal axes of the deposited film and the in-plane vectors of the substrate can be obtained from x-ray pole figure measurement using a four circle x-ray goniometer. The Schultz geometry¹³⁾ is used in this measurement. The α and β rotations are coupled so that a 360° rotation of β corresponds to a 2° increase in α (The θ - 2θ scan corresponds to the case of $\alpha=90^\circ$). A pole figure in Fig. 3(a) shows (117) reflections of BTO grains for a film on LaAlO₃(001). The peaks are located at $\beta=0^\circ, 90^\circ, 180^\circ,$ and 270° with $\alpha \approx 40^\circ$. Since these β positions correspond to the [100] directions of LaAlO₃, the (110) plane of BTO is parallel to the (100) plane of LaAlO₃. Therefore, the BTO films grown on LaAlO₃(001) have an epitaxial growth behavior.

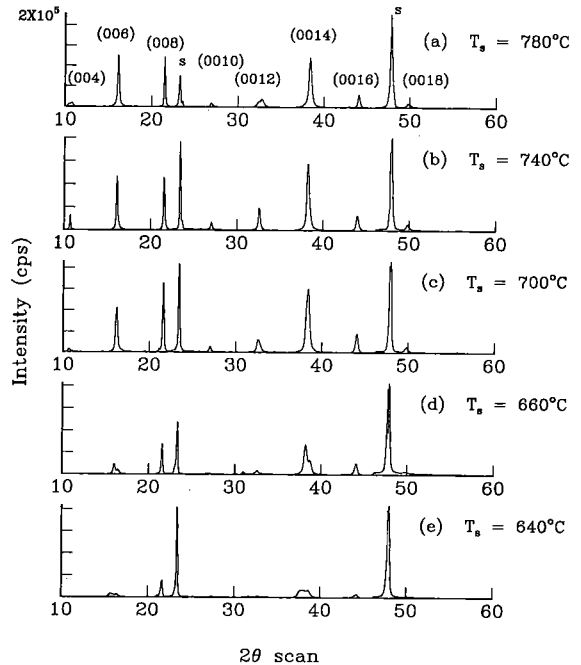


Fig. 2 X-ray diffraction patterns of the BTO thin films on LaAlO₃(001) deposited at (a) 640°C, (b) 670°C, (c) 700°C, (d) 740°C, and (e) 780°C. The character 's' indicates peaks of LaAlO₃.

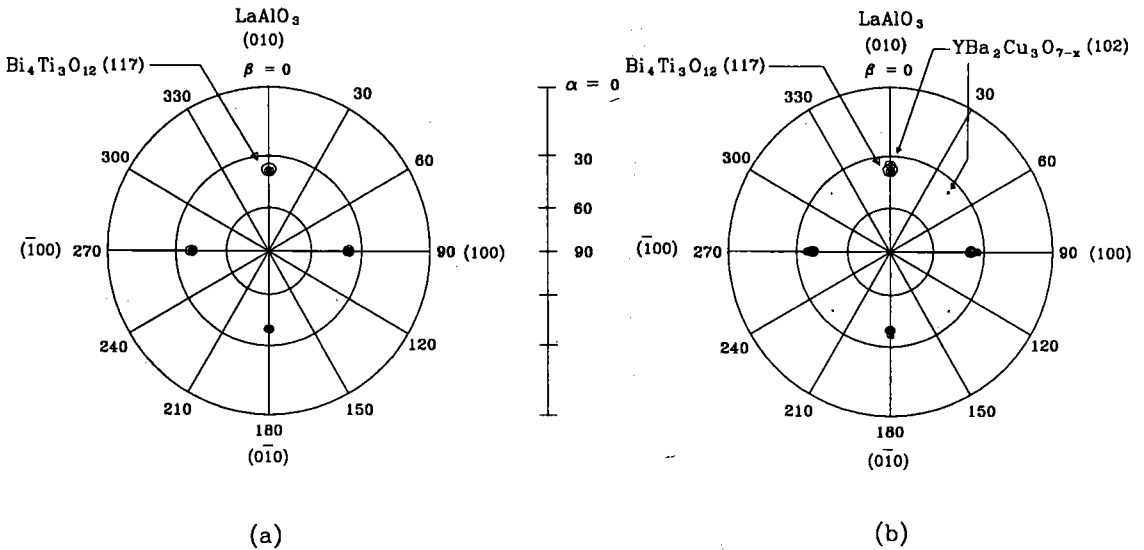


Fig. 3 X-ray pole figures of (a) a BTO/LaAlO₃(001) thin film and (b) a BTO/YBCO/LaAlO₃(001) heterostructure. The pole in Fig. 3(a) represents (117) reflections of BTO grains. In Fig. 3 (b), the poles of BTO(117) and YBCO(102) reflections are plotted.

For the BTO/YBCO/LaAlO₃ heterostructure, a θ - 2θ scan shows that both BTO and YBCO grains are c-axes oriented. A pole figure of the heterostructure is shown in Fig. 3(b). Poles in the figure are (102) reflections of the YBCO grains and (117) reflections of the BTO grains. The YBCO(102) reflections show strong peaks at $\beta = 0^\circ, 90^\circ, 180^\circ$, and 270° and weak peaks at $\beta = 45^\circ, 135^\circ, 225^\circ$, and 315° , with $\alpha \approx 38^\circ$. The ratio between the intensities of these two kinds of peaks is about 10:1. This result indicates that the (100) planes of most YBCO grains are parallel to the (110) planes of LaAlO₃. The (117) reflections of the BTO film show peaks only at $\beta = 0^\circ, 90^\circ, 180^\circ$, and 270° with $\alpha \approx 40^\circ$. Even though the a- and b-axes of the YBCO layer are not perfectly aligned, the BTO grains show epitaxy-like growth behavior such that the

(110) planes of BTO are parallel to the (100) planes of the LaAlO₃ substrate.

The grain growth behavior in the heterostructure can be understood in terms of lattice matching. [The YBCO grains whose (100) planes parallel to the LaAlO₃(110) planes are not considered here.] Lattice constants of LaAlO₃, YBCO, and BTO are shown in Table II. Between room temperature and 675°C , i.e., the ferroelectric Curie temperature of BTO, the a- and b-lattice constants of LaAlO₃ and YBCO are nearly the square roots of those of BTO. Figure 4 illustrates a model of grain growth behavior for the BTO/YBCO/LaAlO₃ heterostructure. The (001) planes of each layer are parallel to each other, i.e., BTO(001)/YBCO(001)/LaAlO₃(001). On the other hand, the (100) planes of most YBCO grains are parallel to the LaAlO₃(100) planes, and the (110)

Table II. Lattice constants of LaAlO₃, YBCO, and BTO. [Reference 14]

Crystal structure		Lattice constants at 30°C (Å)	Lattice constants at 675°C (Å)*
LaAlO ₃	cubic	a=3.79	a=3.81
		a=3.82	a=3.85
YBCO	orthorhombic	b=3.89	b=3.92
		c=11.68	c=11.87
		a=5.41	a=5.45
BTO	monoclinic (pseudo-orthorhombic)	b=5.45	b=5.45
		c=32.82	c=33.17

* 675°C is the ferroelectric Curie temperature of BTO.

planes of all BTO grains are parallel to LaAlO₃(100) planes.

Surface morphology and roughness of the films are investigated with an AFM. An AFM image of the BTO film grown at 740°C is shown in Fig. 5(a). The typical size of the BTO grains is about 1500 Å. Surface morphology of the BTO/YBCO/LaAlO₃ heterostructure is shown in Fig. 5(b). This picture shows boulders on the surface of the heterostructure, which are typical surface irregularities found on most pulsed-laser deposited films.¹⁵⁾ The average

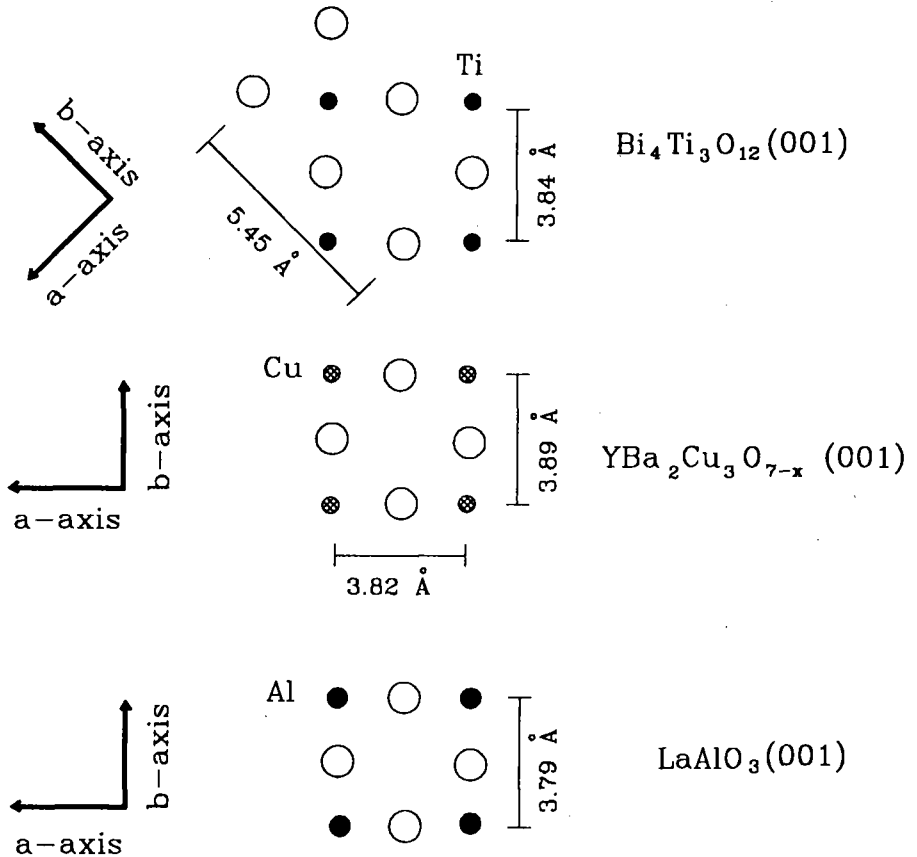
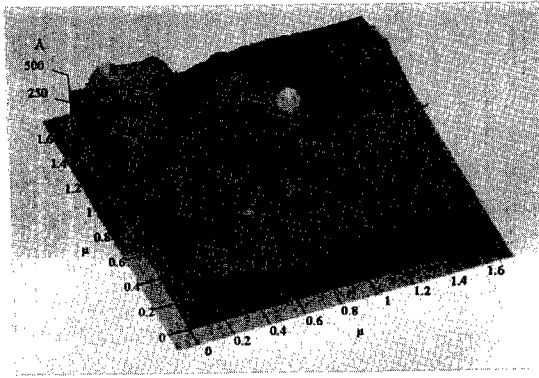
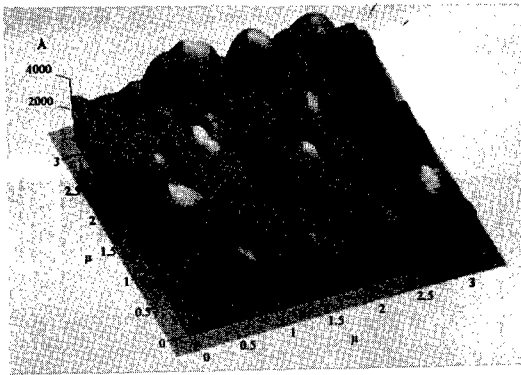


Fig. 4. Surface atomic arrangements of the BTO/YBCO/LaAlO₃ (001) heterostructure. The open circles in the figure represent oxygen atoms of the materials.



(a)



(b)

Fig. 5 AFM micrographs of (a) a BTO/LaAlO₃(001) thin film and (b) a BTO/YBCO/LaAlO₃(001) heterostructure.

size of the boulders is about 5000 Å. The surface of the heterostructure are rougher than that of the BTO film. The surface morphology of laser-ablated YBCO/LaAlO₃(001) was reported elsewhere.¹⁶⁾ The rough surface might come from the insertion of the YBCO layer into the heterostructure. Therefore, the surface morphology of the BTO film in the heterostructure could be improved by growing a smooth YBCO layer on the substrate.

4. Conclusion

BTO thin films are grown on LaAlO₃(001)

substrates by pulsed-laser deposition. The film deposited at 740°C shows an epitaxial growth behavior with its c-axis normal to the substrate. BTO/YBCO/LaAlO₃ heterostructure is *in-situ* grown. It is found that the BTO grains grown on top of the YBCO layer show an epitaxy-like growth behavior even though the a- and b-axes of the YBCO layer are not perfectly aligned to those of LaAlO₃. Therefore, by pulsed-laser deposition it is possible to grow epitaxial BTO thin film on LaAlO₃(001) and YBCO/LaAlO₃(001).

Acknowledgement

This work was supported by the Korea Telecom Research Center (KTRC) and by the Korea Science and Engineering Foundation (KOSEF) through the Science Research Center (SRC) of Excellence Program.

References

1. H. Buhay, S. Sinharoy, W. H. Kasner, M. H. Francombe, D. R. Lampe, and E. Stepke, *Appl. Phys. Lett.* 58, 1470 (1991).
2. W. Jo, G-C. Yi, T. W. Noh, D-K. Ko, Y.S. Cho, and S-I. Kwun, *Appl. Phys. Lett.* 61, 1526 (1992).
3. W. Jo, H-J. Cho, T.W. Noh, B. I. Kim, Z.G. Khim, D-Y. Kim, and S-I. Kwun, *Appl. Phys. Lett.* 63, 2918 (1993).
4. W. Jo, H-J. Cho, T. W. Noh, Y. S. Cho, S-I. Kwun, Y. T. Byun, and S. H. Kim, *Ferroelectrics*, 152, 139 (1994).
5. H-J. Cho, W. Jo, and T. W. Noh, *Appl. Phys. Lett.* 65, 1525 (1994).

6. K. Sugibuchi, Y. Kurogi, and N. Endo, *J. Appl. Phys.* 46, 2877 (1975).
7. S. Y. Wu, W. J. Takei, and M. H. Francombe, *Appl. Phys. Lett.* 22, 26 (1973).
8. J. F. Scott, C. A. Araujo, B. M. Melnick, L. D. McMillan, and R. Zuleeg, *J. Appl. Phys.* 70, 382 (1991).
9. R. Ramesh, W. K. Chan, B. Wilkens, H. Gilchrist, T. Sands, J. M. Tarascon, V. G. Keramidas, D. K. Fork, J. Lee, and A. Safari, *Appl. Phys. Lett.* 61, 1537 (1992).
10. R. Ramesh, A. Inam, B. Wilkens, W. K. Chan, T. Sands, J. M. Tarascon, D. K. Fork, T. H. Geballe, J. Evans, and J. Bullington, *Appl. Phys. Lett.* 59, 1782 (1991).
11. N. J. Wu, A. Ignatiev, A-W. Mesarwi, H. Lin, K. Xie, and H-D. Shih, *Jpn. J. Appl. Phys.* 32, 5019 (1993).
12. S. Ghonge, E. Goo, and R. Ramesh, *MRS Symp. proc.* 243, 399 (1992).
13. T. W. Noh, W. Jo, H-J. Cho, S-H. Lee, T. K. Song, M. S. Ryu, and S-I. Kwun, *J. Kor. Phys. Soc.* 27, S34 (1994).
14. T. Mitsui, et al., *Landolt-Bornstein Vol. 3, Ferroelectric and Antiferroelectric Substance* (Springer-Verlag, New York, 1975), p. 377.
15. G. Koren, A. Gupta, R. J. Baseman, M. I. Lutwyche, and R. B. Laibowitz, *Appl. Phys. Lett.* 55, 2450 (1989).
16. W. Jo, G-C. Yi, D-K. Ko, H. J. Lee, T. W. Noh, Z. G. Khim, and P. H. Hur, *J. Kor. Cer. Soc.* 28, 1005 (1991).